Desalination and Water Treatment
www.deswater.com

doi: 10.5004/dwt.2022.27980

245 (2022) 16–34
January

Uniquely modified polyethersulphone and f-CNTs mixed matrix membranes for enhanced water transport and reduced biofouling

Km Nikita[a], Durga Swetha C.[b], C.N. Murthy[a,*]

[a]*Applied Chemistry Department, Faculty of Technology and Engineering, The Maharaja Sayajirao University of Baroda, Vadodara–390001, India, emails: chivukula_mn@yahoo.com (C.N. Murthy), nikitatiwari.m34@gmail.com (Km Nikita)*
[b]*University at Buffalo, Buffalo, NY, USA 14260-1660, email: chivukula.ds@gmail.com*

Received 24 June 2021; Accepted 3 November 2021

ABSTRACT

Sulfonation of polyethersulfone (SPES) was carried out using chlorosulfonic acid and the modified polymer was then used as a matrix for flat sheet mixed matrix membranes (MMMs). Second component in the MMMs was functionalized multi-walled carbon nanotubes (f-CNTs). The zeta potential study of the cast membranes shows high negative charge on the surface of the membranes containing f-CNTs in comparison to the pristine sulfonated polyethersulfone (SPES) membranes. The addition of carbon nanotubes (CNTs) reduced the roughness parameter of the membranes as revealed by atomic force microscopy study. This also reflected in the reduced irreversible fouling (10.5%). The largest pore size of the membranes having 1.0 wt.% of azide functionalized multi-walled carbon nanotubes was 13.7 nm which classifies them as NF membranes. The highest rejection percentage (91.0%) obtained was for Cu(II) metal by azide functionalized multi-walled carbon nanotubes incorporated membranes. The mechanical stability, in terms of weight loss as observed from thermogravimetric analysis, was the highest as compared to the existing similar membranes with a matching increase in the tensile strength among the membranes of its class.

Keywords: Sulfonated polyethersulfone; Mixed matrix membranes; Small-angle neutron scattering; Carbon nanotubes

1. Introduction

Developments in polymers as membrane materials have been continuously going on since the pioneering work of Bechold (ultrafiltration membranes, 1907) [1], Loeb and Sourirajan (asymmetric membranes, 1960) [2]. The concept of mixed matrix membranes (MMMs) was first introduced by Zimmerman et al., in 1990s to overcome the limitations of polymeric [3] as well as thin-film composite (TFC) membranes [4]. High permeability, enhanced fouling resistance and higher hydrophilicity are the key features of MMMs [5,6]. Unlike the classical polymeric membranes and TFCs, MMMs with higher thermal and mechanical stability offer better compaction properties and can withstand higher pressures. Compaction occurs during the initial stages of membrane operation due to the high pressures involved, which in turn result in an irreversible flux decline [7]. Addition of mechanically strong fillers to the bulk macro void region of asymmetric membranes reduces the structural losses, as the majority of compaction occurs in these regions [8,9].

Both single and multi-walled carbon nanotubes have been used as a second component due to their high mechanical stabilities as well as high surface area and interesting results in water treatment [10] and desalination [11,12] have been observed. There are different studies which have used polyethersulphone (PES) as a polymer matrix for the applications in water treatment [13–15]. To reduce the hydrophobicity of PES, the introduction of the sulfonic acid group on the polymer chain is a modification that is simple and yet effective. Various methods have been

* Corresponding author.

reported for the sulfonation of PES [16–18]. Generally, sulfonate groups can be introduced on the monomer unit of PES: pre-polymerization or post-polymerization. The post-polymerization sulfonation is most frequently used due to the simplicity of the reaction and low cost. Different sulfonation agents such as sulphur-trioxide trimethyl-phosphate complex [12], tri-methyl silyl chloro-sulfonate [16], chlorosulfonic acid [19], and concentrated sulphuric acid [20] have been used in the post-polymerization sulfonation of PES. Since the introduction of the sulfonation reaction of polysulfone by Noshay and Robeson group [21], there have been several studies carried out in this field. This modification led to the improved glass transition temperature (310°C) of the polymer and optimum reverse osmosis desalination (95% salt rejection) results were obtained. In the study, there was no information regarding the pore dimensions of the membranes. In-depth study of sulfonation carried out by Mottet et al. using nuclear magnetic resonance (NMR) spectroscopy showed that only one sulfonic group per aromatic ring can be attached and no other characterization was used in this work [22]. Solvent-free sulfonation was reported by Blanco et al. where sulphuric acid was reacted with polyethersulfone cardo. Sulfonated polymeric membranes showed up to 60% rejection of $CaCl_2$ salt with pure water flux of 1,500 L/m^{2}d. Here too, the pore size of the membranes was not measured. However, the glass transition temperature of the polymer increased after sulfonation [23] which is an indication of lower free volume. Wang et al. have performed sulfonation of PES-cardo using concentrated sulphuric acid varying the degree of sulfonation by controlling the reaction time. The methanol permeability of sulfonated polyethersulfone (SPES)-cardo membranes was found lesser compared to the Nafion® 115 membranes due to difference in their microstructure. No information was given regarding the change in pore size of the membranes after sulfonation was carried out [24]. There are studies where pristine SPES membranes were used as ion exchange membranes [19], as fuel cell membranes [25], and even for pervaporation applications [26]. However, there has been limited work on the use of SPES in the form of MMMs and their application in the liquid separation to the best of our knowledge.

The thin-film composite membranes limitations can be overcome by using the surface-modified MMMs. This modification may include sulfonation of the polyethersulfone backbone which introduces the SO_3H group. These SO_3H groups can be reacted with the amine, azide groups present on nanotubes' surface to form a thin layer on the surface of the polymer without requiring the step of interfacial polymerization.

Herein, we report the novel functionalized MWCNT/SPES MMMs as a strategy to drastically enhance antifouling performance, fouling being the major reason for the continuous development of membrane science specially for water and wastewater treatment. Controlling the degree of sulfonation was an important parameter to devise membranes with tuneable surface properties. Thus, sulfonate groups were first attached to the PES. Using sulfonated polyethersulfone (SPES) and by incorporating functionalized multi-walled carbon nanotubes (f-MWCNTs) in SPES polymer dope solution, using the phase inversion method the MMS were cast. To understand the role of SPES as polymer matrix and f-MWCNTs as the second component for MMMs, the chemical, physical, mechanical properties along with thermal stability of the membranes were probed in detail.

2. Experimental

2.1. Materials

Polyethersulfone (PES) Veradel 3300 was purchased from Permionics Membranes Limited, Vadodara, India. Chlorosulfonic acid, N-methyl pyrrolidone, dichloromethane, isopropanol were purchased from Spectrochem Pvt. Ltd. and used as received. MWCNTs (diameter 6–9 nm) were a commercial-grade sample from Sigma-Aldrich was used as received.

2.2. Sulfonation of polyethersulfone

Polyethersulfone was sulfonated using chlorosulfonic acid (Fig. 1). 20 g of PES dissolved in 400 g of dichloromethane in a round bottom flask, with stirring at room temperature under an inert atmosphere. Subsequently, 15–25 mL of chlorosulfonic acid was added dropwise to the reaction vessel using an addition funnel. The reaction continued for 240 min and then was stopped by dropwise addition of reaction mixture into cold water to get the product. The white precipitates were filtered and washed with deionized (DI) water until the pH became approximately 5–6. Finally, the product was dried at 100°C for 24 h under vacuum. The resulting polymer was used for preparing MMMs using functionalized MWCNTs as the second component.

2.3. Incorporation of f-MWCNT into sulfonated polyethersulfone to form mixed matrix membranes

The nanotubes were functionalized with carboxylic, amide and azide functionalities. The process is described in our previous work [59]. In brief, the unwanted metals and soot were removed from the commercial multi-walled carbon nanotubes to purify it. Further different functional groups (carboxylic, azide and amide) were attached to the purified nanotubes. The SPES was dissolved in N-methyl pyrrolidone to prepare the membrane dope solution and kept under stirring for 24 h for a homogeneous solution. Various wt.% of f-MWCNTs were added to the polymer dope solution followed by sonication for 48h to ensure good dispersion of nanotubes. The composition of membranes is summarized in Table 1. The flat sheet membranes were prepared by phase inversion process using DI water containing 1% isopropanol in the coagulation bath. The membranes were dried under vacuum at 80°C and kept in DI water for further testing (Fig. S1).

2.4. Characterization

2.4.1. Characterization of sulfonated polyethersulfone

Sulfonation of polyethersulfone was test using Fourier transform infrared spectroscopy (FTIR) and nuclear magnetic resonance (NMR) analysis. Thermal stability was

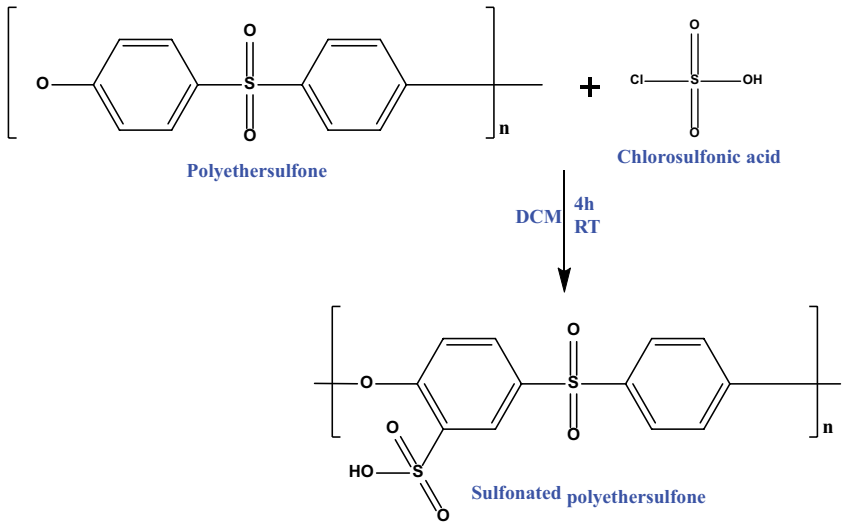

Fig. 1. Schematic representations for the sulfonation of polyethersulfone.

measured by thermogravimetric analysis (TGA). Viscosity of both PES and SPES was measured using a Ubelhode viscometer. The X-ray diffraction study of both polymers has also been carried out.

2.4.2. Characterization of membranes

Membranes were analyzed from field-emission scanning electron microscopy (FE-SEM) to characterize surface and cross-section, contact angle meter utilized to measure surface hydrophilicity of the membranes. TGA was used to analyze thermal stability, small-angle neutron scattering (SANS) technique was applied to explore the arrangement of the pores within the membrane as well as the pore dimensions. Atomic force microscopy (AFM) has given the roughness parameters of the membrane surface.

2.4.3. Fourier transform infrared spectroscopy

FTIR Shimadzu 8400S spectrophotometer was used to detect the functional group associated with the sulphonation of the polymer.

2.4.4. Thermogravimetric analysis

TGA-50 Shimadzu was used to measure the thermal behavior of the polymer and membranes.

2.4.5. Field-emission scanning electron microscopy

Morphology of the membranes was studied by FEG-SEM 450.

2.4.6. Atomic force microscopy

The atomic force microscopy device was NT-MDT-INTEGRA 2005, equipped with Nova 1.0.26.1424 software, utilized to further probe the surface profile of membrane samples in semi-contact mode. Silicon nitride was used as a probe with reflective side as gold. The instrument consists of cantilever/tip assembly that interacts with the samples and the movement of the AFM tip was monitored through a laser beam reflected off the cantilever. Position sensitive photodetector was used to track the reflected laser beam.

Table 1
Composition of membranes

Code	Polymer	f-MWCNT wt.%	Functionality of MWCNT
M1	PES	0	–
S1	SPES	0	–
S201		0.1	Oxidized
S205		0.5	
S21		1	
S301		0.1	Amide
S305		0.5	
S31		1	
S401		0.1	Azide
S405		0.5	
S41		1	

2.4.7. Zeta potential

Zeta potential a measure of electrokinetic potential gives an idea of the surface hydrophilicity is denoted by Greek letter zeta (ζ). The streaming potential E was used to determine the membrane zeta potential using the Helmholtz–Smoluchowski Eq. (1). [21]

$$\zeta = \frac{\Delta E\, \eta\, \lambda}{\varepsilon\, \Delta P} \tag{1}$$

where ΔP is pressure drop across the pore channels, η is the solution viscosity, λ is the solution conductivity and ε is the dielectric constant of the electrolyte solution. Generally,

the separation performance of the membranes is described in terms of size exclusion mechanism but in some cases, the property of electrical double layer near the pore walls is an essential factor of the pore volume. When an electrolyte solution is passed through a capillary under certain pressure an electrical potential is produced which is known as streaming potential. The charge related modification on the surface or inside the pores of the membranes is observed by the evaluation of streaming potential [22].

2.4.8. Contact angle meter

Water contact angle of the surface of the membrane was measured using the model ACAMNSC 03 contact angle meter from Apex Instruments Pvt. Ltd. This was used to measure hydrophilicity of membranes and as a complimentary to information from zeta potential studies. For contact angle, one drop of de-ionized water was taken onto the membrane surface with the help of a syringe and contact angle measured immediately.

2.4.9. Small-angle neutron scattering

The SANS experiments were carried out using SANS diffractometer at Dhruva Reactor, Mumbai, India [23]. The data were collected over the wave vector range ($Q = 4\pi\mathrm{Sin}\theta/\lambda$) of 0.015–0.35 $Å^{-1}$. In this expression, 2θ is the scattering angle, λ is wavelength of incident neutrons. The membranes were cut in small pieces of 1 × 1.5 cm^2 and some few pieces were bundled in an aluminum foil and placed in the path of the neutron beam. Analysis of the data was done after it was corrected for direct beam and the background contribution.

2.4.10. Tensile test

Tensile strength in the dry state was measured at room temperature using Lloyd LRX instrument at a speed of 2 mm/min and gauge length 14 mm. The membrane stripes were of 5 cm length with thickness between 0.12–0.23 mm.

2.5. Rejection and fouling experiments

All rejection and fouling measurements were carried out in a stainless-steel test cell fabricated in house with an effective membrane area of 50 cm^2. Commercial booster pump was used for the circulation of feed solution in the setup. The concentrate outlet valve was utilised to control the volumetric flow rate and trans membrane pressure. The stabilization of the membrane was carried out at 71 psi (4.8 bar) pressure 2 h at before the experiment. The pure water flux was measured at two different pressures 71 and 98 psi (6.7 bar). The permeate flux of all the membrane sample was calculated by using Eq. (2).

$$J_1 = \frac{W}{A\Delta t} \tag{2}$$

where W is the volume of permeate at time Δt and A is membrane area.

The percent rejection of heavy metals and bovine serum albumin (BSA) was calculated using Eq. (3).

$$\text{Rejection}\,(\%) = \frac{C_f - C_p}{C_f} \times 100 \tag{3}$$

where C_f and C_p denote the concentration of feed and permeate respectively. Atomic absorption spectrometer (AAS) (Analytikjena Nova-400) was used to measure the metal concentration in the permeate. Measurement of mercury and arsenic was performed using graphitic furnace mode of AAS while other metals were analysed in the flame mode. All measurements were performed with single beam AAS equipped with 100 mm burner, across flow nebulizer 5.0 mL/min and 1.2 mm slit were used. Each measurement was repeated twice to reduce the error margins. Shimadzu-2450 UV Spectrometer was used to measure the concentration of BSA feed and permeate solution.

The fouling of membranes was measured with 500 ppm aqueous solution of BSA. Subsequently, the membranes were backwashed with deionised water for 30 min and pure water flux of the cleaned membranes (J_2) was measured. The flux recovery ratio (FRR) and irreversible fouling ratio (R_{ir}) of the membranes were calculated by below mentioned Eqs. (4) and (5) respectively.

$$\text{Flux recovery ratio}\,(\%) = \frac{J_2}{J_1} \times 100 \tag{4}$$

$$\text{Irreversible fouling ratio}\,(\%) = \frac{J_1 - J_2}{J_1} \times 100 \tag{5}$$

where J_1 is pure water flux of membrane and J_2 is pure water flux of cleaned membrane after rejection experiment is done and J_3 is the protein filtration flux.

3. Results and discussion

3.1. Characterization of SPES/f-MWCNT membranes

3.1.1. Fourier transform infrared spectroscopy

The substitution of SO_3H group to the polyethersulfone was established using FTIR analysis. On comparing the FTIR spectra of SPES and PES shown in Fig. 2, the appearance of the band at 3,444 cm^{-1} in SPES spectra were attributed to the stretching of hydroxyls of sulfonic acid groups and the absorption peak that appeared at 1,027 cm^{-1} was the characteristic of aromatic SO_3H symmetric stretching vibrations [27]. Other signals were common in both spectra, signals at 1,327 and 1,297 cm^{-1} are due to asymmetric O=S=O stretching of sulfone group; peak at 1,247 cm^{-1} corresponds to asymmetric O–C–O stretching of aryl ether group; signal at 1,148 cm^{-1} was for symmetric stretching of sulfone group; signals at 1,107 and 1,072 cm^{-1} were for aromatic ring vibrations; at 1,077 cm^{-1} signal for vibrations of aromatic ring bonded to sulfonate group appears [23,24,28]. This confirms the attachment of the sulfonic acid group to the polymer chain.

3.1.2. Nuclear magnetic resonance (NMR) spectroscopy

3.1.2.1. ^1H NMR

The substitution of the sulfonic acid group to the benzene ring of polyethersulfone was confirmed from NMR

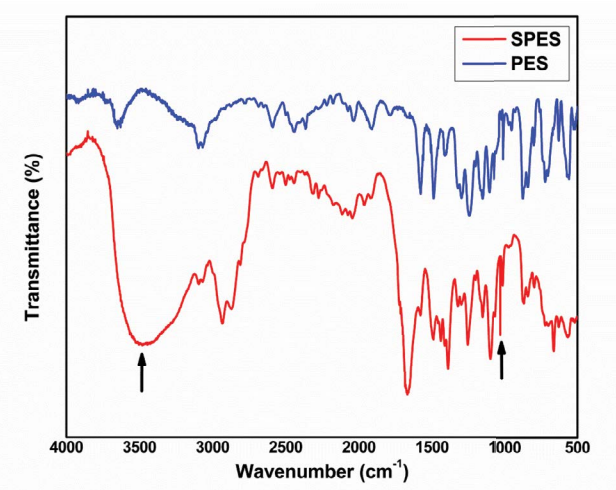

Fig. 2. FTIR spectra of polyethersulfone (PES) and sulfonated polyethersulfone (SPES).

spectroscopy. As can be seen from the ^{1}H NMR spectra, a significant downfield shift from 7.2 to 8.3 ppm of the hydrogen marked as H_d at the aromatic ringin the SPES structure (Figs. 3, S2 and S3) occurs due to the presence of sulfonic acid group which was in agreement with previously reported studies [22,29–31].

3.1.3. Thermogravimetric analysis

The thermal stability of SPES was determined by thermogravimetric analysis. In the SPES sample decomposition at three different temperature ranges can be seen in Fig. 4. The first decomposition occurred at around 100°C, which is related to the loss of water bonded to a sulfonic acid group. The second degradation takes place at around 400°C, which is due to the decomposition of sulfonic acid groups. The third decomposition at around 480°C is attributed to the degradation of the polymer main chain. However, PES polymer shows only one sharp degradation at around 540°C, which is assigned to the polymer main chain degradation. Also, the lower thermal stability of SPES could be due to the enhanced asymmetry in PES structure which is attributed to the addition of sulfonic acid group that makes it less regular, hence less stable [27,32].

3.1.4. Viscosity measurement and degree of sulfonation

Viscosity study was performed to identify probable chain scission during the sulfonation process. As shown in Table 2, the sulfonated polyethersulfone had inherent viscosity value equal to 1.84 dL/g which was greater than the parent polyethersulfone. These results indicate that there is no chain cleavage or degradation of the original polymer due to sulfonating agent [26]. The intrinsic viscosity of SPES sample had increased compared to the value for PES, possibly due to the enhancement of interchain interactions which results in higher resistance to the stretching of the main chains because of the attachment of SO_3H group [32]. The degree of sulfonation was calculated by acid-base titration. The predetermined amount of sulfonated

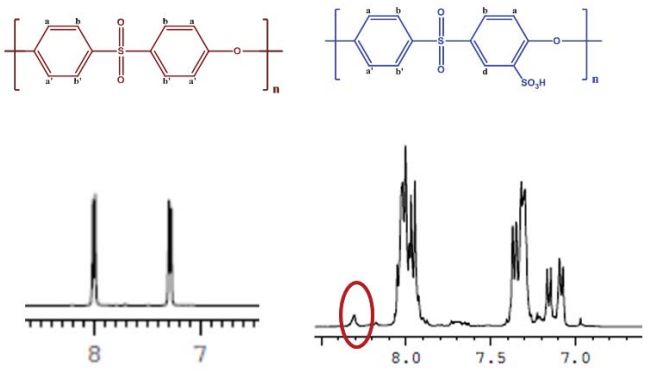

Fig. 3. ^{1}H NMR spectra of PES and SPES polymer.

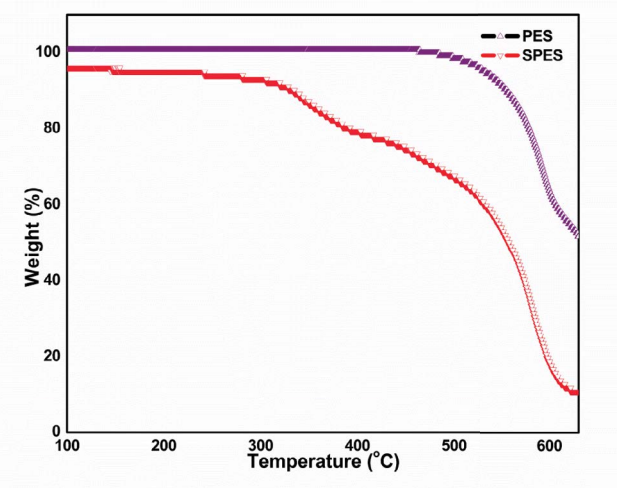

Fig. 4. TGA spectra of polyethersulfone and sulfonated polyethersulfone.

PES was mixed with a quantized amount of solvent NMP, 2–3 drops of 0.1% phenolphthalein indicator solution was added into this solution before titrating it with a standardized NaOH aqueous solution. The obtained value for the SPES sample was 30.2%.

3.1.5. X-ray diffraction

X-ray diffraction analysis has been performed to evaluate the structural aspect of the post sulfonation of the polymer. The data of the X-ray diffraction analysis of polyethersulfone (PES) and sulfonated polyethersulfone (SPES) is summarized in Table 3. Both the polyethersulfone and sulfonated polyethersulfone have shown the characteristic of amorphous polymer [33]. The data were compared in terms of peak position, peak intensity and d-spacing. The peak intensity decreased in SPES compared to PES which implies reduced macromolecular orientation within the polymer.

3.2. Characterization of SPES/f-MWCNT membranes

3.2.1. Field-emission scanning electron microscopy

The polymer films were cast on a glass plate. The surface of the SPES as well as f-MWCNT containing MMMs were

Table 2
Viscosity values for polyethersulfone and sulfonated polyethersulfone in solvent NMP at 30°C

	η_{sp}	η_{int}
PES	1.12	1.72
SPES	1.24	1.84

Table 3
X-ray diffraction values of PES and SPES

	2θ (°)	Peak intensity (counts per second)	d-spacing (Å)
PES	21.07	452.19	4.21
SPES	19.7	274	4.49

observed using field emission scanning electron microscopy. The surface morphology is showing the smooth surface and there is not much change in morphology with the addition of functionalized nanotubes (Figs. 5 and S4).

The membranes were freeze fractured in liquid nitrogen and cross-section viewed under an FE-SEM. The cross-section of the 1.0 wt.% Am-MWCNT/SPES membranes showed the finger-like macro voids (Fig. S5). The addition of MWCNT in the polymer matrix changed membrane upper layer by eliminating the wider layer and there is the formation of a thin skin layer on the membrane surface.

3.2.2. Atomic force microscopy

The AFM images of pristine PES, pristine SPES, Az-MWCNT/SPES membranes are shown in Figs. 6 and S6, which revealed that membrane surface roughness mainly depends on the composition of the casting solution. In case of pristine PES and pristine SPES, the surface roughness of the membrane with sulfonated polyethersulfone is higher which can be explained as the SPES being hydrophilic thus enhanced affinity of SPES/NMP casting solution towards water coagulation bath compared to PES/NMP dope solution, leading to a lower mutual diffusion rate between the solvent NMP and non-solvent water. This delayed mutual diffusion allowed longer time for phase inversion and thus segregation of smaller amount of SPES from bulk casting solution up to the solution water interface, resulting in a rougher surface [34]. Average roughness value for PES is 9.21 nm which is increased to 11.02 nm for SPES membranes. Furthermore, the different loadings of functionalized nanotubes enhanced the interaction between SPES matrix and nanotubes thus segregation of SPES is reduced which resulted in the formation of smooth membrane surface (Table 4). This enhanced smoothness facilitates the frictionless flow of water through the membrane pores which gives higher pure water flux (PWF). The highest PWF showed by 0.1% Az MWCNT/SPES membrane (450.7 LMH). However, pristine sulfonated polyethersulfone (SPES) with higher surface roughness showed more PWF than pristine polyethersulfone (PES) membrane which is attributed to larger pore size. Thus, both the pore size and roughness are responsible for the alteration of PWF values.

3.2.3. Contact angle

The limitation of polyethersulfone membranes is their hydrophobic nature which gives rise to fouling of the membrane, thus reducing the life of the membranes [35,36]. The contact angle of sulfonated polyethersulfone membrane and functionalized nanotubes containing MMMs are measured to observe the change in the surface properties and hydrophilicity. The contact angle values are given in Tables 5 and S2. Pristine SPES membranes are having 49.13°, which is the indication of improved hydrophilicity of the membrane due to sulfonation of PES. The lower contact angle, that is, higher hydrophilicity of SPES membranes may be accredited to the polar groups of SPES polymer, having SO_3H groups which are strongly hydrophilic.

Table 4
Roughness parameters of pristine PES [M1], pristine SPES [S1], 0.1 wt.% Az-MWCNT/SPES [S401], 0.5 wt.% Az-MWCNT/SPES [M405], 1.0 wt.% Az-MWCNT/SPES [M41] MMMs

	Average roughness Sa (nm)	Root mean square Sq (nm)
M1	9.21	11.41
S1	11.02	14.35
S401	4.02	5.09
S405	4.87	6.61
S41	4.17	5.33

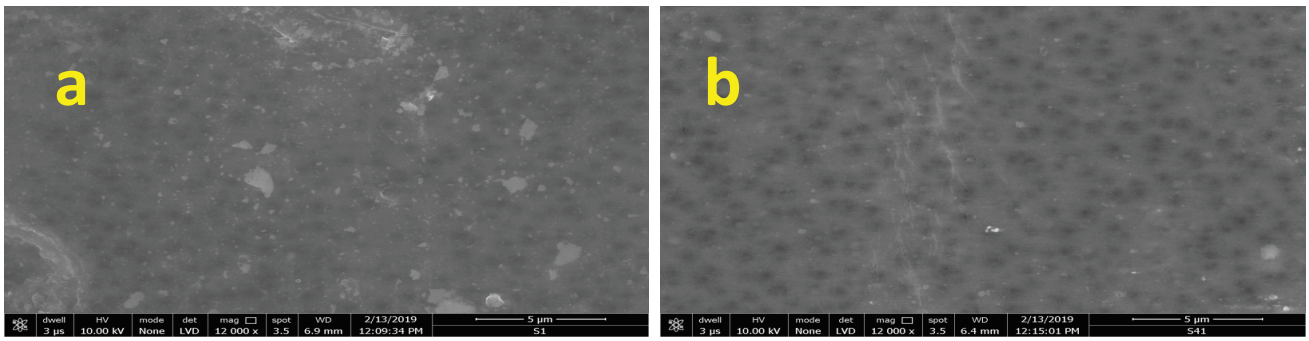

Fig. 5. FE-SEM image of the surface of the pristine SPES (a) 1.0 wt.% Ox-MWCNT/SPES and (b) 1.0 wt.% Am-MWCNT/SPES.

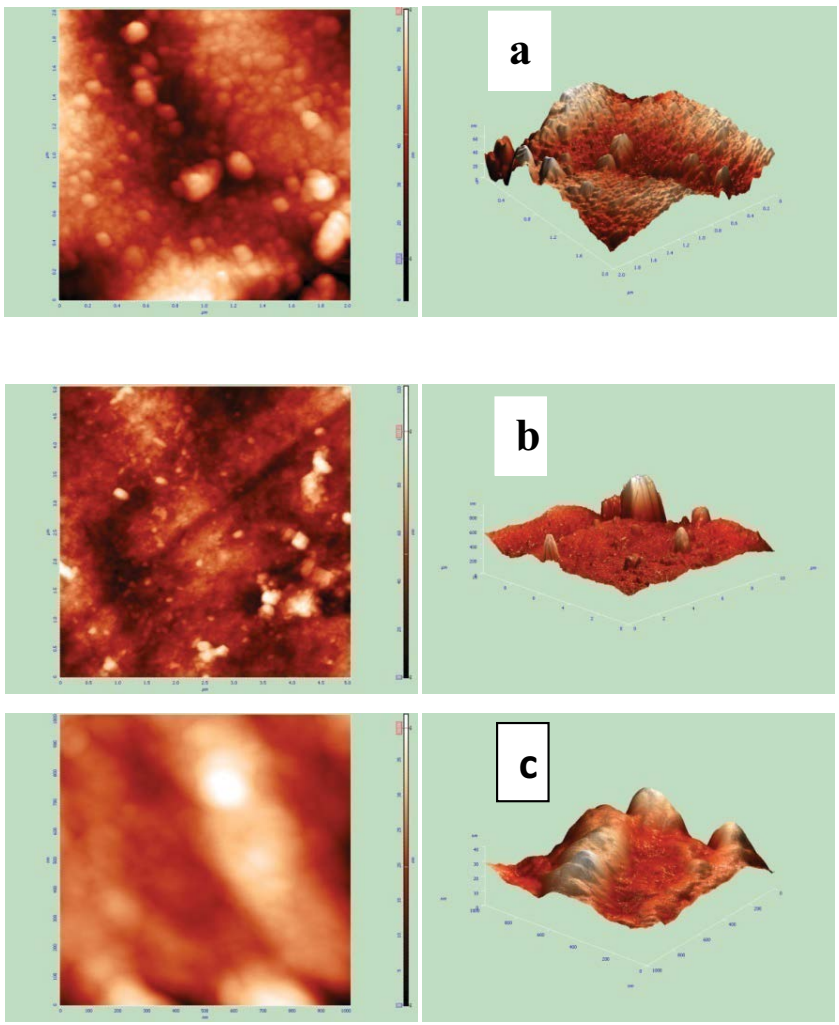

Fig. 6. AFM images of (a) pristine PES, (b) pristine SPES and (c) 1.0 wt.% Az-MWCNT/SPES.

The contact angles are much reduced for the MMMs containing f-MWCNT and reached to the value of 38.84° for 1 wt.% Az-MWCNT/SPES membranes. Furthermore, for all the functionality of nanotubes, the contact angle is decreased with increasing the content of nanotubes in the polymer matrix.

3.2.4. Zeta potential measurement

The evaluation of the charge generated on the membrane surface is a vital parameter to understand the antifouling performance of the membranes. The sulfonated PES membranes are retaining negative charge on the membrane surface as in case of PES membranes (Fig. 7a), however, the SPES membranes are showing higher negative charge which is in agreement with previous report [37–41]. The MMMs containing oxidized, amide and azide MWCNT are showing negative zeta potential in the pH range of 2.5–7.0 (Fig. 7b) and no isoelectric point could be observed. The negative charge is decreasing at the lower pH value.

The membranes show higher surface negative charge when compared to other functionalized polysulfone/nanocomposite combinations (Table 6).

Table 5
Contact angle values of pristine SPES and f-MWCNT/SPES MMMs

Code	Contact angle (°)
M1	73.3 ± 3.0
S1	49.13 ± 1.3
S21	39.47 ± 1.7
S31	39.70 ± 1.2
S41	38.84 ± 1.0

3.2.5. Small-angle neutron scattering

SANS is the technique to probe the morphology of the porous materials. In this technique, wave properties of the neutron are used to probe the structure of the material. Detailed discussion regarding the principle of the instrument is already described in the previous section. Corrections were performed through the whole duration of data analysis for instrumental smudging. The calculated scattering profiles were smeared by the appropriate resolution function to

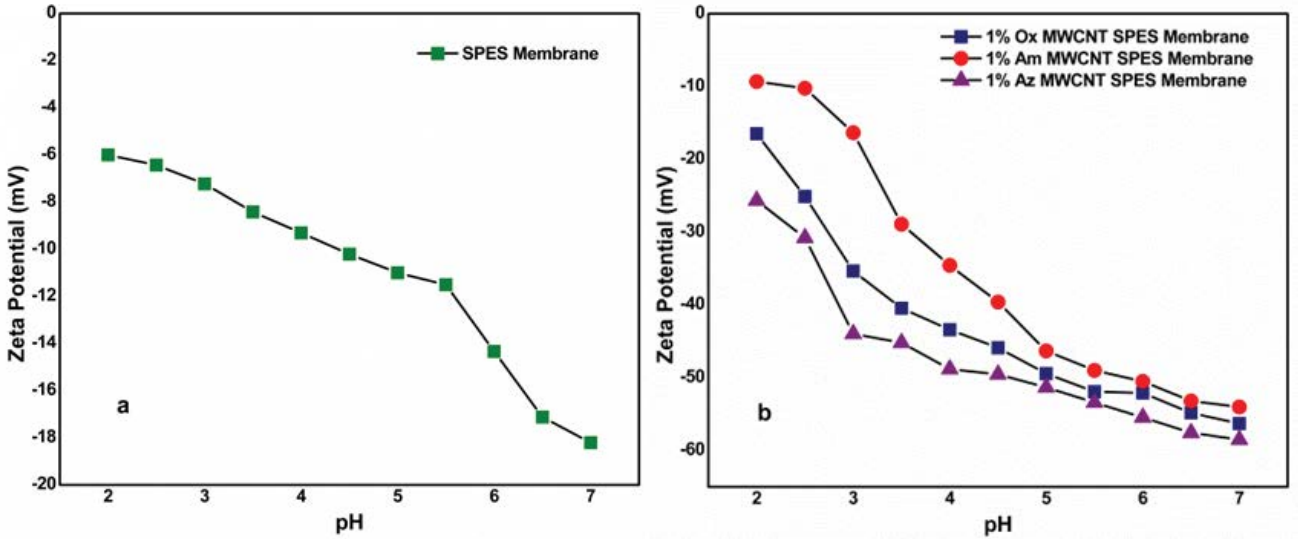

Fig. 7. The zeta potential value of (a) SPES and (b) mixed matrix membranes as a function of pH.

compare with the measured data. The SANS profile of pristine SPES membrane and 0.1, 0.5 and 1 wt.% all the functionalized (oxidized, amide and azide) MWCNT MMMs are shown in Fig. 8, respectively.

The data was interpreted using SASFIT software. Two different models were considered: (i) the polydisperse sphere model where the pores are taken to be spherical surrounded by the matrix material and (ii) the random two-phase model, where the first phase is the pores and the second phase is the matrix material surrounding the pores. Our data was giving a better fit to the second model, which confirms the presence of nanotubes in the polymer matrix.

The correlation length of pristine SPES membrane, as well as MMMs, prepared from sulfonated SPES is 3.9 nm (Tables 7 and S1), which is identical to the correlation length of PES membranes. This implies that the porosity of SPES membranes is decreased as the correlation length considered to be distance between the pores. The pore size of the azide functionalized MWCNT/SPES membranes is least, thus giving the best filtration results.

3.2.6. Thermogravimetric analysis

The TGA plots of SPES and SPES/f-MWCNT MMMs showed three-step weight degradation (Fig. 9). The first weight loss was between 100°C to 190°C which was ascribed to the loss of water attached to the hygroscopic sulfonic acid group. The second degradation was observed at around 400°C which may be due to the decomposition of the sulfonic acid group. The third weight loss was at around 500°C which was attributed to the polymeric backbone degradation. The thermal stability of SPES membrane was improved with the addition of azide functionalized MWCNT fillers in different weight percentage [0.1 wt.% (S401), 0.5 wt.% (S405) and 1 wt.% (S41)].

From the Table 8, it is observed that unlike other doping materials, when SPES is doped with MWCNTs, the thermal stability of the membrane increases drastically. Unless the mother liquor in which the polymer is dissolved is varied, the thermal stability of the membrane doesn't drastically vary from the 300°C temperature mark. This is indicative of the fact, that the introduction of the MWCNTs, which have a higher thermal stability, have aided in the thermal stability of these new membranes.

Table 6
Comparative study of zeta potentials of polyethersulfone membranes

Membranes	Zeta potential values	Reference
SPES/PANi	–50	[38]
PES/SPES blend	–60	[39]
PES/POT	–30	[40]
SPES/NH_2	–45	[41]
SPES/f-CNTs	–55	This work

Table 7
SANS of membrane soaked in D_2O

Code	Pore radius (nm)	Polydispersity (σ)	Correlation length (nm)
M1	14.8	0.27	3.9
S1	15.4	0.25	3.9
S21	14.1	0.27	3.9
S31	14.0	0.29	3.9
S41	13.7	0.30	3.9

3.2.7. Tensile strength

The durability of the mixed matrix membrane widely gets affected by mechanical failure [46]. The tensile properties of the membranes were evaluated by performing tensile strength test. The tensile strength was improved as compared to the bare SPES membrane. When using different functionalized nanotubes as fillers in the polymer matrix

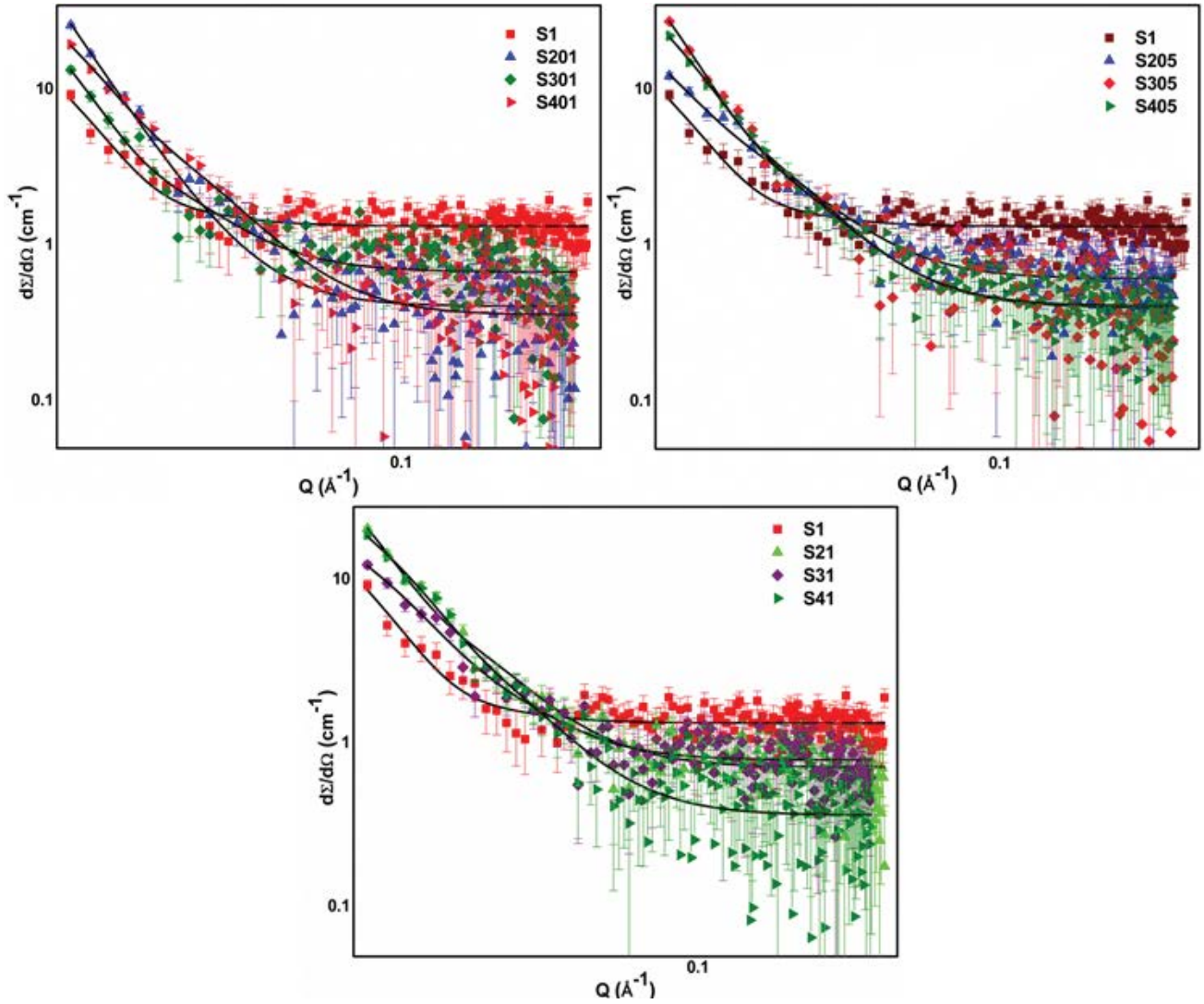

Fig. 8. SANS profile of membranes soaked in D_2O.

Table 8
Comparison of thermal stability of the new membrane to literature

Membranes	First mass loss temperature	Reference
SPES/Az-MWCNT (1 wt.%)	439	This work
SPES/SiO_2 (3 wt.%)	307	[42]
SPES (30% sulfonation)	400	[27]
SPES/PWA-silica	320	[43]
SPES/DMAc/PEG200	500.8	[44]
SPES/Ga_2O_3 (3 wt.%)	320	[45]

the tensile strength varies and the highest was in the case of azide functionalized MWCNT. Stress vs. strain curve is shown in Fig. 10. The SPES, 1.0 wt.% Ox-MWCNT/SPES, 1.0 wt.% Am-MWCNT/SPES and 1.0 wt.% Az-MWCNT/SPES membrane samples can withstand elongation at

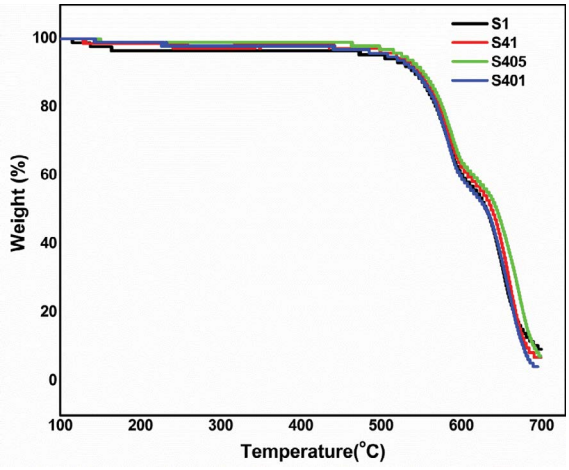

Fig. 9. TGA curves of SPES membrane and 0.1 wt.% Az-MWCNT/SPES (S401), 0.5 wt.% Az-MWCNT/SPES (S405), 1 wt.% Az-MWCNT/SPES (S41) mixed matrix membranes.

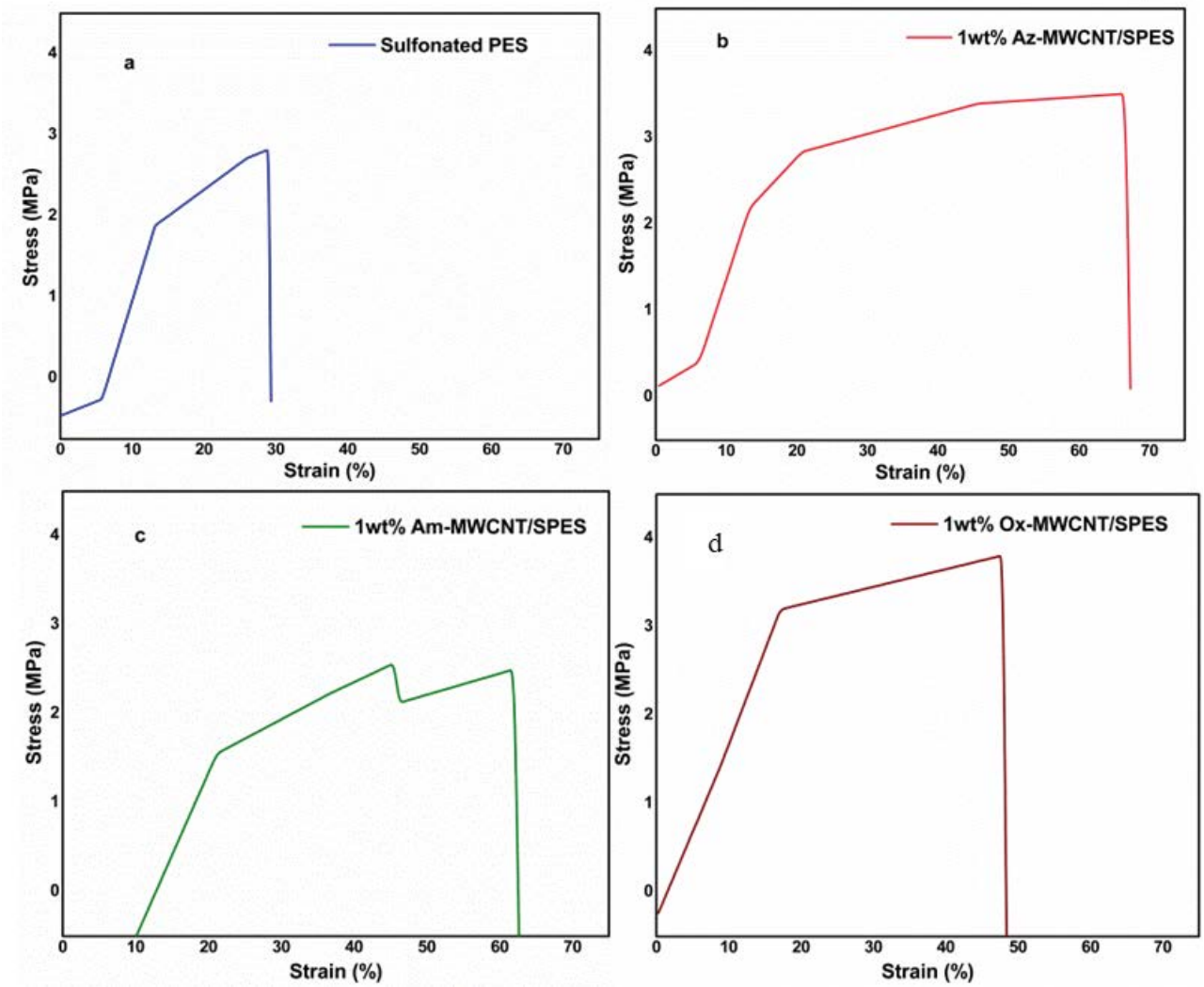

Fig. 10. Stress vs. strain curve of (a) pristine SPES, (b) 1.0 wt.% Az-MWCNT/SPES membranes, (c) 1.0 wt.% Am-MWCNT/SPES and (d) 1.0 wt.% Ox-MWCNT/SPES.

break up till 28.7%, 47.5%, 61.75% and 65.9%, respectively. The maximum stress that the membranes can withstand is 2.78 MPa for pristine sulfonated SPES, 3.78 MPa for oxidized, 2.46 MPa for amide and 3.48 MPa for azide membranes.

As evidenced from the Table 9, the MWCNTs in the membrane matrix have aided the tensile strength of the membranes. Most of the other nanoparticles don't show much deviation from the pristine membrane. It can also be observed that the variation in the sulfonation of the PES effects the mechanical strength of the membrane. In this work, the higher sulfonation of the membrane had a positive effect on the membrane properties. It can also be observed that membranes that included other polymeric substitutes have higher tensile strength, however, it is evident that the membranes were quite brittle by looking at the elongation percentage.

3.2.8. Permeation studies of f-MWCNT/SPES membranes

The effect on pure water permeation by using sulfonated polyethersulfone as a polymer matrix and f-MWCNT as filler was also studied. The pure water flux was measured at different pressure and varying pH. When the polymer matrix was replaced by SPES the pure water flux values are summarized in Table 10. It is seen that the pure water flux of SPES membrane was enhanced compared to the PES membrane and this could be due to the enhanced hydrophilicity of the membranes since the addition of SO_3H group to the PES.

The pure water flux of SPES membrane was increased in comparison to the PES membrane (Fig. 11). As revealed by SANS study the pore size of the SPES membrane was increased, and hydrophilicity of the SPES membrane was also enhanced as measured by contact angle meter. These two combined effects are probably the reason behind the enhancement in pure water flux [50]. In case of the MMMs having f-MWCNT in the polymer matrix, the pure water flux keeps on increasing compared to SPES membrane, due to the enhanced hydrophilicity and bigger pore size of membranes (Fig. 12 and Table S3). In addition to this, the pure water flux was also improved due to the presence

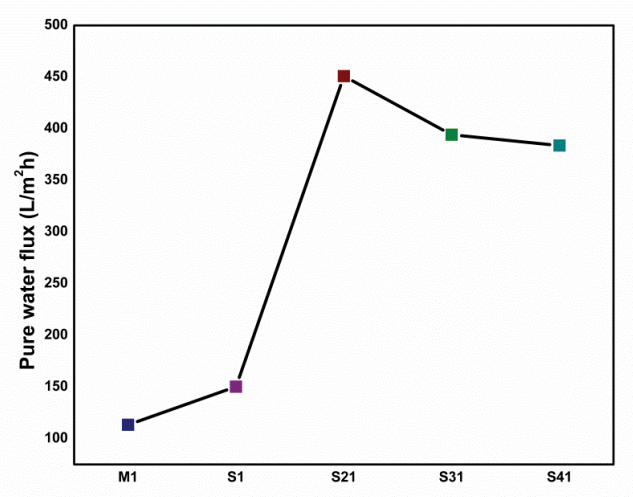

Fig. 11. Pure water flux values of f-MWCNT/SPES membranes.

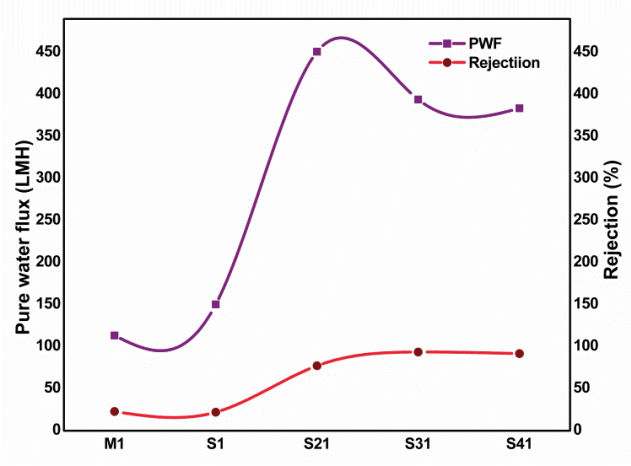

Fig. 12. Pure water flux and Cu(II) metal rejection of pristine PES (M1), pristine SPES (S1), 1% oxidized MWCNT/SPES (S21), 1% amide functionalized MWCNT/SPES (S31) and 1% azide functionalized MWCNT/SPES (S41) membranes.

of functionalized nanotubes which provides frictionless transport of water through the nanotube channels [50,51].

3.2.9. Heavy metal removal studies of SPES/f-MWCNT membranes

Feed solutions were prepared by dissolving the appropriate amount of compound to the DI water. We have prepared feed solution of 1 ppm concentration. Stock solution of chromium and lead are prepared by dissolving 2.84 g of $K_2Cr_2O_7$ and 1.59 g of $Pb(NO_3)_2$ in 1,000 mL of DI water. Cadmium solution was prepared by dissolving 1 g of cadmium salt in a minimum volume of HCl and then making it up to 1,000 mL with DI water. Feed solution of copper and arsenic were prepared of 1,000 mg/L concentration with the respective metal salts. The experiment was carried out in the membrane filtration setup fabricated in-house. The filtration experiment was carried out at 25°C temperature. The Az-MWCNT/SPES membranes were tested at two pressure 71 and 98 psi to observe the effect on rejection by enhancing pressure. Cr(VI), Pb(II), Cu(II) are the metals which were selected for analyzing the pressure effect. The rejection (%) of Cr(VI), Pb(II), Cu(II) at 71 psi were 19.4, 18.9, 22.1 for pristine SPES membrane, which was reduced to 16.9, 15.6 and 20.4 respectively at 98 psi pressure. The same phenomenon occurred for the rest of the MMMs having Az-MWCNT as fillers, the values are summarized in Table 11. On augmenting of pressure, the rejection percentage of metals decreased, this was probably due to the enhanced flow rate of permeate [52–54]. This observation is in line with the observations of Kook et al., in their work on transport through polymeric membranes [55]. In the work, Kook et al., reported that as the flux increased due to increase in pressure, there is membrane deformation that led to increased flux; however, the salt rejection was observed to be decreased.

The filtration experiment was also carried out at acidic as well as neutral pH for Cr(VI) metal. The pH was maintained at 2.5 by the addition of HCl solution to the Cr(VI) feed solution. The effect of pH on the rejection of Cr(VI) metal is shown in Fig. 13.

For mixed matrix membrane having 0.1, 0.5 and 1.0 wt.% Az-MWCNT, Cr(VI) rejection was 64.5, 71.1, 76.1 respectively at 2.5 pH which was reduced to 51.3, 62.1, 69.8 respectively in a neutral environment. The removal of chromium was higher at acidic pH as compared to neutral pH; this is in agreement with the result mentioned by Anah et al. [56]. Thus, the optimum condition could be obtained as 2.5 pH and 71 psi pressure for metal removal studies.

The filtration experiment has been performed for different weight percentage of Ox, Am and Az-MWCNT incorporated SPES MMMs. The rejection of nanotube incorporated mixed matrix SPES membrane was higher than the pristine SPES membrane due to the active sites present at membranes because of functionalized nanotubes. On increasing the functionalized nanotubes concentration

Table 9
Tensile strength comparison of our membrane with those in literature

Membranes	Tensile strength (MPa)	Elongation (%)	Reference
SPES/Az-MWCNT (1 wt.%)	3.8	65.9	This work
SPES/DMAc/PEG200	2.49	26.0	[44]
SPES/$SMoS_2$	1.52	53.9	[47]
SPES/PEI	1.34	20.1	[48]
CS-PVA-SPES (5 wt.%)	4	1.6	[49]

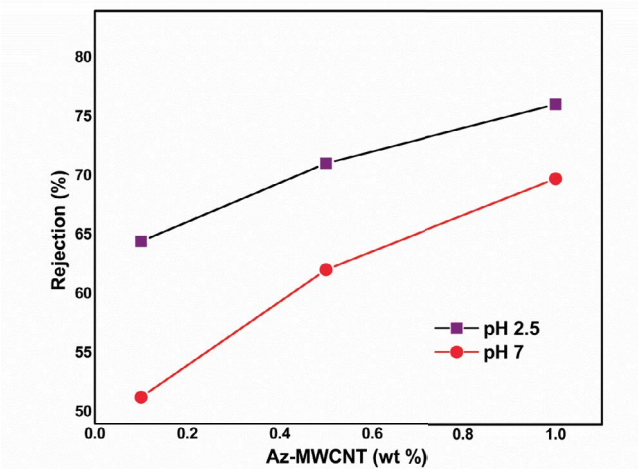

Fig. 13. Percentage removal of Cr(VI) at different pH at 71 psi pressure.

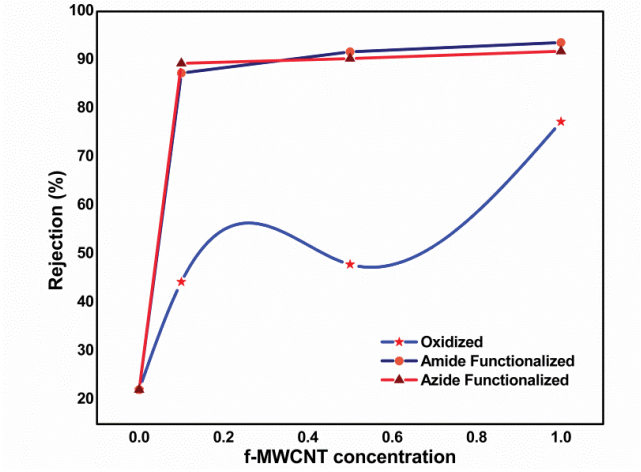

Fig. 14. Effect of functionality and concentration of nanotubes on Cu(II) metal rejection.

into the membrane matrix, the rejection percentage keeps on increasing, this may be accredited to the reduced pore size, enhanced number of active sites on MWCNTs due to functionalization. The metal removal was found to be more prominent in the case of azide (Table 14) and amide (Table 13) group containing membranes (Fig. 14). The azide and amide groups were probably having a better metal binding capacity in comparison to the carboxylic group and hence 78.7% As and 91.8% Cu was rejected from azide MWCNT/SPES MMM, while only 74.5% As and 77.3% Cu rejection was obtained from oxidized MWCNT/SPES MMM (Table 12).

In the case of azide MWCNT/SPES MMM, 0.1% azide gave 87.3% Cu(II) rejection while 1% azide has given 91.8% rejection. With the increased concentration of nanotubes, the pore dimension is decreased resulting higher flux as compared to pristine SPES membrane, thus giving better removal of heavy metal ions and could be considered as most suitable for metal removal out of other MMMs. On the other hand, virgin SPES membrane gave very less rejection. Virgin SPES membrane gave 22.1% Cu rejection, which is very less as compared to MMMs.

3.2.10. Fouling studies of SPES/f-MWCNT membranes

The pure water flux was first measured and then feed tank was refilled with 500 ppm BSA solution. After BSA filtration the pure water was passed through the membrane for 1 h and then pure water was filled as feed to determine the fouling, after which the flux with the cleaned membrane represented as J_2 was measured. The protein rejection was measured by Eq. (3). To appraise the resistive ability of the modified membranes against fouling, flux recovery ratio (FRR) is calculated by Eq. (4). The fouling process was studied in detail, some more expressions of irreversible fouling ratio (R_{ir}) was calculated according to Eq. (5). The results obtained are summarized in Tables 15 and S4.

Accumulation of the foulants on the membrane cause fouling of membranes, thus the interaction between foulant and the membrane surface govern the antifouling performance of the membranes [56]. The recycling properties of

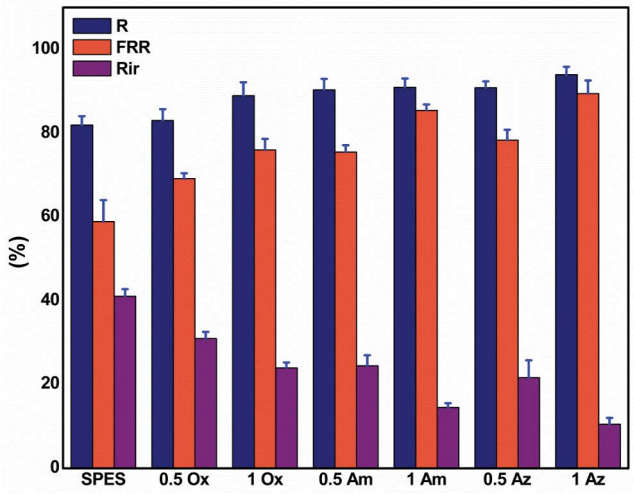

Fig. 15. Representation of BSA rejection (R), flux recovery ratio (FRR), irreversible fouling ratio (R_{ir}) of SPES and f-MWCNT/SPES MMMs.

the membranes can be shown by flux recovery ratio (Fig. 15). The enhanced FRR indicates the better antifouling properties of the membranes. The FRR of the virgin SPES membrane is 58.9 ± 5.1 which is higher than the value for PES membrane (54.3 ± 6.1). The enhancement is FRR is probably due to the better hydrophilicity of the SPES membrane than PES membrane which is confirmed by the contact angle measurement. In the same way, the addition of f-MWCNT to the SPES polymer matrix further reduce the contact angle and thus increased FRR value. It is observed that on increasing the weight percentage of functionalized nanotubes, the FRR value increases. And out of three functionality azide functionalized membranes shows the best antifouling properties. The highest value of FRR is 89.5 ± 3.1 for the Az-MWCNTs 1 wt.% membrane.

Membranes fouling comprise reversible fouling ratio and irreversible fouling ratio. Monolayer of protein adsorption on the membrane surface causes irreversible fouling which

Table 10
Pure water flux values of the membranes at different pressures

Code	Pure water flux (L/m²h)	
	71 psi	98 psi
M1	113.36	124.62
S1	150.30	165.30
S21	450.9	480.00
S31	394.15	407.92
S41	383.71	399.91

Table 11
Metal ions rejection for azide functionalized MWCNT/SPES membranes at pressure 71 and 98 psi and at pH 2.5

Code	Removal capacity (%)					
	Cr(VI)		Pb(II)		Cu(II)	
	71 psi	98 psi	71 psi	98 psi	71 psi	98 psi
M1	20.0	17.1	19.0	16.3	22.9	21.3
S1	19.4	16.9	18.9	15.6	22.1	20.4
S401	64.5	56.1	54.8	43.5	79.3	70.2
S405	71.1	62.4	64.7	50.9	90.3	81.3
S41	76.1	65.2	70.7	61.6	91.8	79.6

Table 12
Metal ions rejection at pH 2.5 for oxidized MWCNT/SPES membranes at 71 psi pressure

Code	Removal capacity (%)				
	Cr(VI)	Pb(II)	Cd(II)	Cu(II)	As(III)
M1	20.0	19.0	20.5	22.9	18.3
S1	19.4	18.9	19.8	22.1	18.5
S201	30.9	23.1	48.9	44.3	50.9
S205	48.8	28.6	53.9	47.9	54.7
S21	59.4	37.2	65.4	77.3	74.5

Table 13
Metal ions rejection at pH 2.5 for amide functionalized MWCNT/SPES membranes at 71 psi pressure

Code	Removal capacity (%)				
	Cr(VI)	Pb(II)	Cd(II)	Cu(II)	As(III)
M1	20.0	19.0	20.5	22.9	18.3
S1	19.4	18.9	19.8	22.1	18.5
S301	63.9	53.6	74.7	87.3	73.9
S305	68.8	64.1	77.6	91.7	79.4
S31	74.3	67.5	78.9	93.6	81.5

Table 14
Metal ions rejection at pH 2.5 for azide functionalized MWCNT/SPES membranes at 71 psi pressure

Code	Removal capacity (%)				
	Cr(VI)	Pb(II)	Cd(II)	Cu(II)	As(III)
M1	20.0	19.0	20.5	22.9	18.3
S1	19.4	18.9	19.8	22.1	18.5
S401	64.5	54.8	72.2	89.3	73.7
S405	71.1	64.7	75.2	90.3	76.1
S41	76.1	70.7	76.8	91.8	78.7

Table 15
BSA rejection and fouling ratio of the SPES/f-MWCNT MMMs

Code	Bovine serum albumin		
	Rejection (%)	Flux recovery ratio (%)	Irreversible fouling ratio (%)
M1	84.0 ± 2.1	54.3 ± 6.1	45.7 ± 1.7
S1	82.0 ± 2.1	58.9 ± 5.1	41.1 ± 1.7
S21	89.0 ± 3.2	76.1 ± 2.6	23.9 ± 1.3
S31	91.0 ± 2.1	85.5 ± 1.4	14.5 ± 1.0
S41	94.0 ± 1.9	89.5 ± 3.1	10.5 ± 1.5

cannot be removed by simple water flushing due to the strong adsorption. However, deposition of proteins on the adsorbed layer gives rise to of reversible fouling since these proteins are loosely attached, which can be removed by simple hydraulic cleaning [57,58].

The lowest value of irreversible fouling ratio is for 1 wt.% azide MWCNTs membrane (10.5 ± 1.3) which is probably because of excellent dispersion of nanotubes and enhanced hydrophilicity thus avoiding the direct contact between protein molecules and the membrane [59,60]. Hence protein molecule can be removed by simple water washing. However, the irreversible fouling ratio is also significant for the 1 wt.% amide MWCNTs membrane (14.5 ± 1.5). As azide membranes are giving better rejection, they are most suitable for several runs of protein filtration.

From the Fig. 16, it can be concluded that though both amide functionalized CNT-SPES membrane and azide functionalized CNT-SPES have similar Cu(II) rejections, the flux recovery of azide is better than amide and the pure water flux of amide is better than azide. This indicates that the usage of azide in more fouling feed water would be profitable in comparison to other membranes detailed in this report.

4. Conclusions

This study explored the outcome of functionalized multi-walled carbon nanotubes on the morphology and rejection performance of f-CNTs/SPES mixed matrix membranes. With the above-mentioned results, the rejection efficiencies of f-CNTs/SPES MMMs have to be explored to determine a targeted area of application. The negatively charged membrane surface indicates that these membranes are resistant to fouling and would best utilised in desalination, waste-water treatment, bio and gas sensors where the highest bio fouling takes place. The addition of f-CNTs

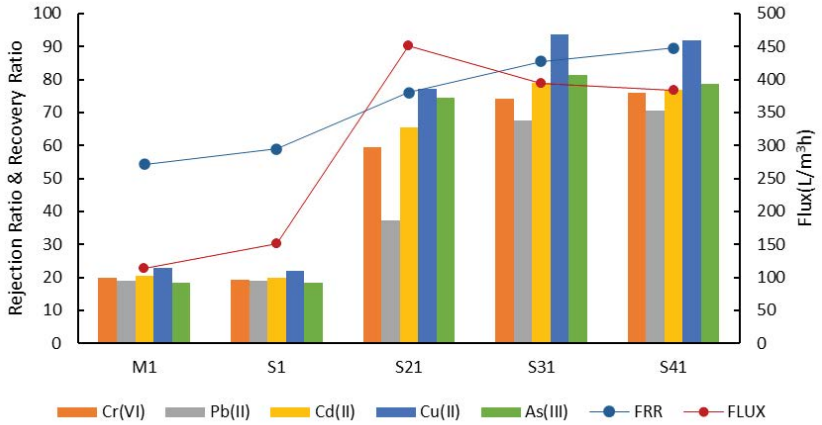

Fig. 16. Flux, flux recovery and rejection behavior of different membranes.

improved the hydrophilicity and tensile strength of mixed matrix membranes. The sulfonate moiety has increased the surface charge of the pristine SPES as well as SPES MMMs which support the antifouling nature of the membranes. The degree of sulphonation has potential to tune the antifouling property of the resulting NF MMMs. Out of the other mentioned functional groups in the manuscript, azide functionalized CNT-SPES have comparable Cu(II) rejections, though the flux recovery of azide is better. This makes azide CNTs/SPES most suitable for the much fouled feed solution.

References

[1] H. Bechhold, Kolloidstudien mit der Filtrationsmethode, Zeitschrift für Elektrotechnik und Elektrochemie, 13 (1907) 527–533.

[2] S. Loeb, S. Sourirajan, Sea water demineralization by means of an osmotic membrane, Adv. Chem., 38 (1963) 117–132.

[3] C.M. Zimmerman, A. Singh, W.J. Koros, Tailoring mixed matrix composite membranes for gas separations, J. Membr. Sci.,137 (1997) 145–154.

[4] J. Alam, L.A. Dass, M. Ghasemi, M. Alhoshan, Synthesis and optimization of PES-Fe_3O_4 mixed matrix nanocomposite membrane: application studies in water purification, Polym. Compos., 34 (2013) 1870–1877.

[5] Y. Yang, H. Zhang, P. Wang, Q. Zheng, J. Li, The influence of nano-sized TiO_2 fillers on the morphologies and properties of PSF UF membrane, J. Membr. Sci., 288 (2007) 231–238.

[6] Y. Li, G. He, S. Wang, S. Yu, F. Pan, H. Wu, Z. Jiang, Recent advances in the fabrication of advanced composite membranes, J. Mater. Chem. A,1 (2013) 10058–10077.

[7] K.M. Persson, V. Gekas, G. Trägårdh, Study of membrane compaction and its influence on ultrafiltration water permeability, J. Membr. Sci., 100 (1995) 155–162.

[8] G. Jonsson, Methods for determining the selectivity of reverse osmosis membranes, Desalination, 24 (1977) 19–37.

[9] L. Zhang, J. Xu, Y. Tang, J. Hou, L. Yu, C. Gao, A novel long-lasting antifouling membrane modified with bifunctional capsaicin-mimic moieties via in situ polymerization for efficient water purification, J. Mater. Chem. A, 4 (2016) 10352–10362.

[10] A.R. Boroujeni, M. Karimi, M. Javanbakht, Application of novel surface-modified PES membranes for removal of heavy metals from aqueous solutions, Desal. Water Treat., 57 (2016) 19794–19809.

[11] M. Peydayesh, T. Mohammadi, O. Bakhtiari, Water desalination via novel positively charged hybrid nanofiltration membranes filled with hyperbranched polyethyleneimine modified MWCNT, J. Ind. Eng. Chem., 69 (2019) 127–140.

[12] L. Wang, X. Song, T. Wang, S. Wang, Z. Wang, C. Gao, Fabrication and characterization of polyethersulfone/carbon nanotubes (PES/CNTs) based mixed matrix membranes (MMMs) for nanofiltration application, Appl. Surf. Sci., 330 (2015) 118–125.

[13] A. Rahimpour, M. Jahanshahi, N. Mortazavian, S.S. Madaeni, Y. Mansourpanah, Preparation and characterization of asymmetric polyethersulfone and thin-film composite polyamide nanofiltration membranes for water softening, Appl. Surf. Sci., 256 (2010) 1657–1663.

[14] H. Abdallah, A. El-Gendi, M. Khedr, E. El-Zanati, Hydrophobic polyethersulfone porous membranes for membrane distillation, Front. Chem. Sci. Eng.,9 (2015) 84–93.

[15] A. Rahimpour, S.S. Madaeni, M. Jahanshahi, Y. Mansourpanah, N. Mortazavian, Development of high performance nanoporous polyethersulfone ultrafiltration membranes with hydrophilic surface and superior antifouling properties, Appl. Surf. Sci.,255 (2009) 9166–9173.

[16] M.S. Kang, Y.J. Choi, I.J. Choi, T.H. Yoon, S.H. Moon, Electrochemical characterization of sulfonated poly(arylene ether sulfone) (S-PES) cation-exchange membranes, J. Membr. Sci., 216 (2003) 39–53.

[17] J.F. Blanco, Q.T. Nguyen, P. Schaetzel, Sulfonation of polysulfones: suitability of the sulfonated materials for asymmetric membrane preparation, J. Appl. Polym. Sci., 84 (2002) 2461–2473.

[18] C. Iojoiu, M. Maréchal, F. Chabert, J.-Y. Sanchez, Mastering sulfonation of aromatic polysulfones: crucial for membranes for fuel cell application, Fuel Cells, 5 (2005) 344–354.

[19] C. Klaysom, B.P. Ladewig, G.Q.M. Lu, L. Wang, Preparation and characterization of sulfonated polyethersulfone for cation-exchange membranes, J. Membr. Sci., 368 (2011) 48–53.

[20] S.W. Lin, F.J. Lopez-Garcia, S. Perez-Sicairos, R.M. Felix-Navarro, New method of synthesis of sulfonated polyethersulfone (SPES) and effect of pH on synthetic gray water filtration performance by negatively charged SPES/PS UF membranes, Desal. Water Treat., 57 (2016) 24807–24819.

[21] A. Noshay, L.M. Robeson, Sulfonated polysulfone, J. Appl. Polym. Sci., 20 (1976) 1885–1903.

[22] C. Mottet, A. Revillon, P. Le Perchec, M.F. Llauro, A. Guyot, Analogous reaction for maximum sulfonation of polysulfones, Polym. Bull., 8 (1982) 511–517.

[23] J.F. Blanco, Q.T. Nguyen, P. Schaetzel, Novel hydrophilic membrane materials: sulfonated polyethersulfone, J. Membr. Sci., 186 (2001) 267–279.

[24] L. Li, Y. Wang, Sulfonated polyethersulfone Cardo membranes for direct methanol fuel cell, J. Membr. Sci., 246 (2005) 167–172.

[25] N.N. Krishnan, D. Henkensmeier, J.H. Jang, H.J. Kim, V. Rebbin, I.H. Oh, S.A. Hong, S.W. Nam, T.H. Lim, Sulfonated poly(ether sulfone)-based silica nanocomposite membranes for high

temperature polymer electrolyte fuel cell applications, Int. J. Hydrogen Energy, 36 (2011) 7152–7161.
[26] I. Byun, I. Kim, J. Seo, Pervaporation behavior of asymmetric sulfonated polysulfones and sulfonated poly(ether sulfone) membranes, J. Appl. Polym. Sci., 76 (2000) 787–798.
[27] R. Guan, H. Zou, D. Lu, C. Gong, Y. Liu, Polyethersulfone sulfonated by chlorosulfonic acid and its membrane characteristics, Eur. Polym. J., 41 (2005) 1554–1560.
[28] B.C. Johnson, I. Yilgor, C. Tran, M. Iqbal, J.P. Wightman, D.R. Lloyd, J.E. McGrath, Synthesis and characterization of sulfonated poly(acrylene ether sulfones), J. Polym. Sci. A, 22 (1984) 721–737.
[29] R. Nolte, K. Ledjeff, M. Bauer, R. Mülhaupt, Partially sulfonated poly(arylene ether sulfone) – a versatile proton conducting membranes material for modern energy conversion technologies, J. Membr. Sci., 83 (1993) 211–220.
[30] I.C. Kim, J.G. Choi, T.M. Tak, Sulfonated polyethersulfone by heterogeneous method and its membrane performance, J. Appl. Polym. Sci., 74 (1999) 2046–2055.
[31] H. Dai, R. Guan, C. Li, J. Liu, Development and characterization of sulfonated poly(ether sulfone) for proton exchange membrane materials, Solid State Ionics, 178 (2007) 339–345.
[32] F. Lufrano, I. Gatto, P. Staiti, V. Antonucci, E. Passalacqua, Sulfonated polysulfone ionomer membranes for fuel cells, Solid State Ionics, 145 (2001) 47–51.
[33] L. Unnikrishnan, S.K. Nayak, S. Mohanty, G. Sarkhel, Polyethersulfone membranes: the effect of sulfonation on the properties, Polym. Plast. Technol. Eng., 49 (2010) 1419–1427.
[34] H. Wu, X. Li, C. Zhao, X. Shen, Z. Jiang, X. Wang, Chitosan/sulfonated polyethersulfone−polyethersulfone (CS/SPESPES) composite membranes for pervaporative dehydration of ethanol, Ind. Eng. Chem. Res., 52 (2013) 5772–5780.
[35] Y. Osada, T. Nakagawa, Membrane Science and Technology, CRC Press, 1992.
[36] Y. Mansourpanah, S.S. Madaeni, M. Adeli, A. Rahimpour, A. Farhadian, Surface modification and preparation of nanofiltration membrane from polyethersulfone/polyimide blend-use of a new material (polyethyleneglycol-triazine), J. Appl. Polym. Sci., 112 (2009) 2888–2895.
[37] W. Zhao, Q. Mou, X. Zhang, J. Shi, S. Sun, C. Zhao, Preparation and characterization of sulfonated polyethersulfone membranes by a facile approach, Eur. Polym. J., 49 (2013) 738–751.
[38] H. Nagar, N. Sahu, V.V. Basava Rao, S. Sridhar, Surface modification of sulfonated polyethersulfone membrane with polyaniline nanoparticles for application in direct methanol fuel cell, Renewable Energy, 146 (2020) 1262–1277.
[39] L.F. Fang, H.Y. Yang, L. Cheng, N. Kato, S. Jeon, R. Takagi, H. Matsuyama, Effect of molecular weight of sulfonated poly(ether sulfone) (SPES) on the mechanical strength and antifouling properties of poly(ether sulfone)/SPES blend membranes, Ind. Eng. Chem. Res., 56 (2017) 11302–11311.
[40] M. Alhoshan, J. Alam, A. Khan, F. Surur Al Shabouna, S. Sasivarnam, L. Arockiasamy Dass, A.K. Shukla, Polysulfone–poly(orthotoluidine) nanocomposite membrane with an improved separation performance, Polym. Compos., 38 (2017) E157–E166.
[41] J. Zhu, Q. Zhang, S. Li, S. Zhang, Fabrication of thin film composite nanofiltration membranes by coating water soluble disulfonated poly(arylene ether sulfone) and in situ crosslinking, Desalination, 387 (2016) 25–34.
[42] S. Wen, C. Gong, W.C. Tsen, Y.C. Shu, F.C. Tsai, Sulfonated poly(ether sulfone)/silica composite membranes for direct methanol fuel cells, J. Appl. Polym. Sci., 116 (2010) 1491–1498.
[43] C.C. Chen, H.Y. Tsi, W.C. Tsen, F.S. Chuang, S.C. Jang, Y.C. Shu, S. Wen, C. Gong, PWA/silica doped sulfonated poly(ether sulfone) composite membranes for direct methanol fuel cells, J. Appl. Polym. Sci., 123 (2012) 1184–1192.
[44] M. Liu, A.L. Skov, S.H. Liu, L.Y. Yu, Z. liang Xu, A facile way to prepare hydrophilic homogeneous PES hollow fiber membrane via non-solvent assisted reverse thermally induced phase separation (RTIPS) method, Polymers, 11 (2019) 269, doi: 10.3390/polym11020269.
[45] S. Miao, H. Zhang, Z. Chen, B. Wang, X. Li, Y. Wu, Sulfonated polyarylene ether sulfone (SPES) and Ga_2O_3 based hybrid polymer electrolyte membrane for direct methanol fuel cells (DMFCs), Chem. Res. Chin. Univ., 32 (2016) 318–324.
[46] A. Kusoglu, A.M. Karlsson, M.H. Santare, S. Cleghorn, W.B. Johnson, Mechanical behavior of fuel cell membranes under humidity cycles and effect of swelling anisotropy on the fatigue stresses, J. Power Sources, 170 (2007) 345–358.
[47] V. Yadav, N. Niluroutu, S.D. Bhat, V. Kulshrestha, Sulfonated poly(ether sulfone) based sulfonated molybdenum sulfide composite membranes: proton transport properties and direct methanol fuel cell performance, Mater. Adv., 1 (2020) 820–829.
[48] N. Harsha, S. Kalyani, V.V. Basava Rao, S. Sridhar, Synthesis and characterization of polyion complex membranes made of aminated polyetherimide and sulfonated polyethersulfone for fuel cell applications, J. Fuel Cell Sci. Technol., 12 (2005) 061004.
[49] S. Meenakshi, S.D. Bhat, A.K. Sahu, P. Sridhar, S. Pitchumani, A.K. Shukla, Chitosan-polyvinyl alcohol-sulfonated polyethersulfone mixed-matrix membranes as methanol-barrier electrolytes for DMFCs, J. Appl. Polym. Sci., 124 (2011) E73–E82.
[50] A. Rahimpour, S.S. Madaeni, S. Ghorbani, A. Shockravi, Y. Mansourpanah, The influence of sulfonated polyethersulfone (SPES) on surface nano-morphology and performance of polyethersulfone (PES) membrane, Appl. Surf. Sci., 256 (2010) 1825–1831.
[51] M. Majumder, N. Chopra, R. Andrews, B.J. Hinds, Enhanced flow in carbon nanotubes, Nature, 438 (2005) 44.
[52] P. Shah, C.N. Murthy, Studies on the porosity control of MWCNT/polysulfone composite membrane and its effect on metal removal, J. Membr. Sci., 437 (2013) 90–98.
[53] K. Nikita, P. Karkare, D. Ray, V.K. Aswal, P.S. Singh, C.N. Murthy, Understanding the morphology of MWCNT/PES mixed-matrix membranes using SANS: interpretation and rejection performance, Appl. Water Sci., 9 (2019) 154.
[54] K. Nikita, D. Ray, V.K. Aswal, C.N. Murthy, Surface modification of functionalized multi-walled carbon nanotubes containing mixed matrix membrane using click chemistry, J. Membr. Sci., 596 (2020) 117710.
[55] S. Kook, C.D. Swetha, J. Lee, C. Lee, T. Fane, I.S. Kim, Forward osmosis membranes under null-pressure condition: do hydraulic and osmotic pressures have identical nature?, Environ. Sci. Technol., 52 (2018) 3556–3566.
[56] L. Anah, N. Astrini, Influence of pH on Cr(VI) ions removal from aqueous solutions using carboxymethyl cellulose-based hydrogel as adsorbent, IOP Conf. Ser.: Earth Environ. Sci., 60 (2017) 012010.
[57] E. Celik, H. Park, H. Choi, H. Choi, Carbon nanotube blended polyethersulfone membranes for fouling control in water treatment, Water Res., 45 (2011) 274–282.
[58] V. Vatanpour, S.S. Madaeni, R. Moradian, S. Zinadini, B. Astinchap, Novel antibifouling nanofiltration polyethersulfone membrane fabricated from embedding TiO_2 coated multi-walled carbon nanotubes, Sep. Purif. Technol., 90 (2012) 69–82.
[59] Km Nikita, S. Kumar, V.K. Aswal, D.K. Kanchan, C.N. Murthy, Porous structure studies of the mixed-matrix polymeric membranes of polyethersulfone incorporated with functionalized multi-walled carbon nanotubes, Desal. Water Treat., 146 (2019) 29–38
[60] E. Celik, L. Liu, H. Choi, Protein fouling behaviour of carbon nanotube/polyethersulfone composite membranes during water filtration, Water Res., 45 (2011) 5287–5294.

Supporting information

In the 13C NMR spectra of SPES (Figs. S2 and S3), some additional signals were present which was present due to the sulfonic acid bonded to the benzene rings influencing the chemical shifts of neighboring carbon atoms, compared to the 13C spectra of PES [1].

Table S1
SANS data of membrane soaked in D_2O

Sample	Pore radius (nm)	Polydispersity (σ)	Correlation length (nm)
S201	15.2	0.24	3.9
S205	14.7	0.25	3.9
S301	14.8	0.26	3.9
S305	14.3	0.28	3.9
S401	13.7	0.30	3.9
S405	13.7	0.30	3.9

Table S2
Contact angle values of pristine SPES and f-MWCNT/SPES mixed matrix membranes

Membranes	Contact angle (°)
S201	41.51 ± 2.4
S205	40.72 ± 3.1
S301	43.69 ± 5.2
S305	41.11 ± 2.9
S401	40.75 ± 3.0
S405	40.56 ± 1.1

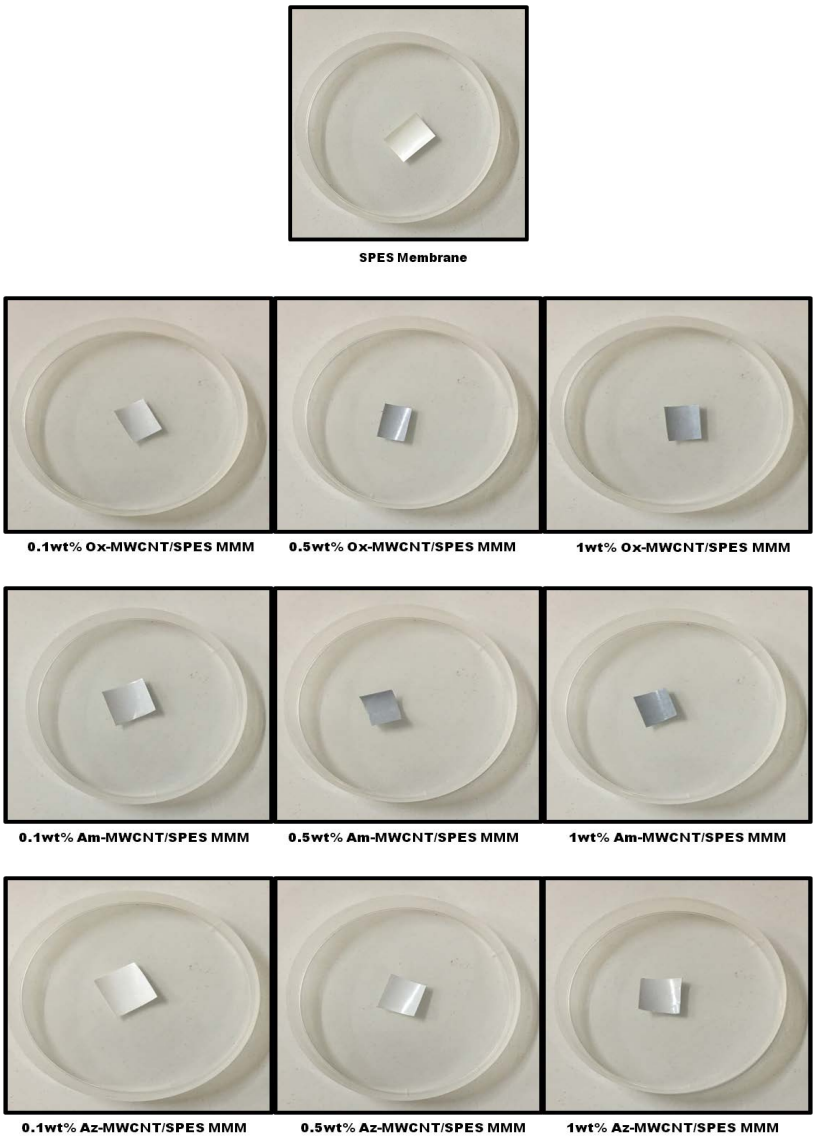

Fig. S1. Images of prepared pristine SPES and f-MWCNT/SPES mixed matrix membranes.

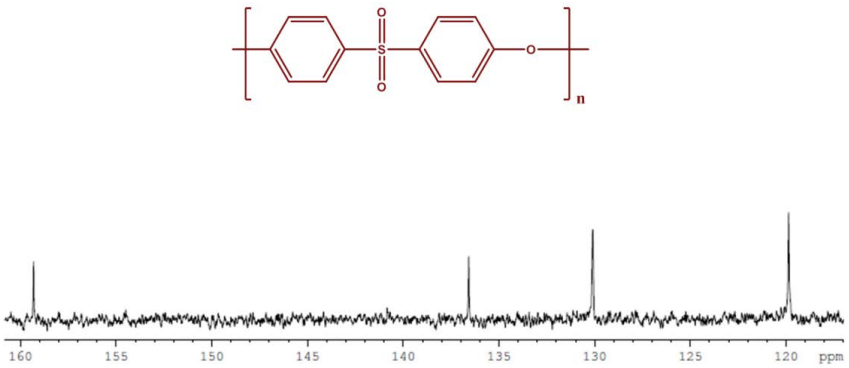

Fig. S2. 13C NMR spectra of polyethersulfone polymer.

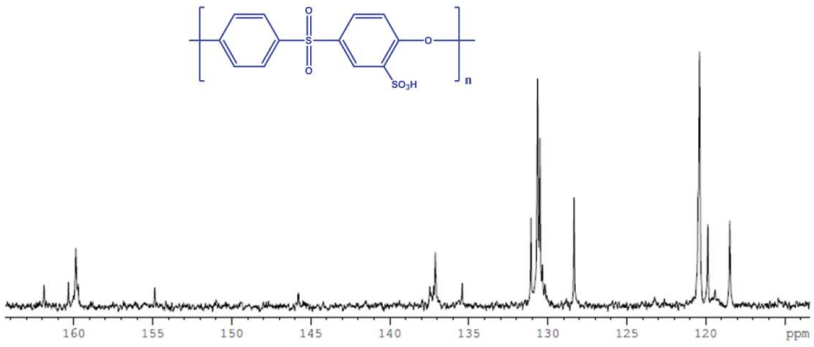

Fig. S3. 13C NMR spectra of sulfonated polyethersulfone polymer.

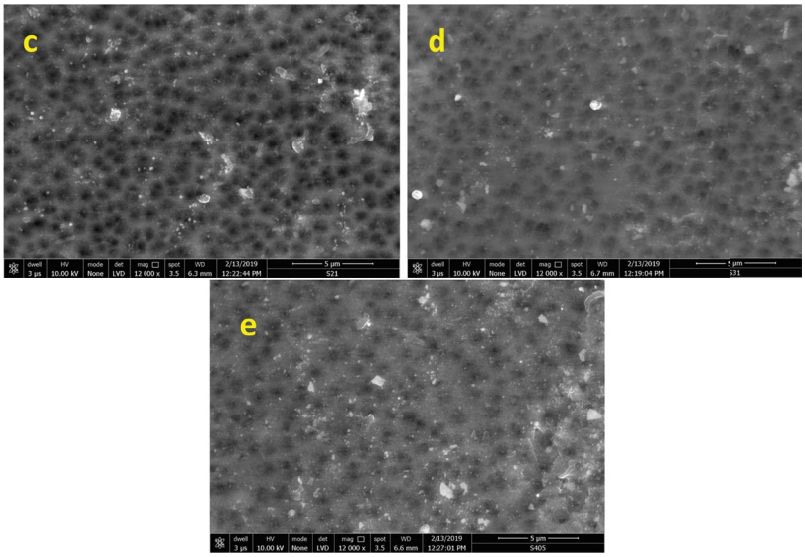

Fig. S4. FE-SEM image of the surface of 1 wt.% Ox-MWCNT/SPES (c), 1 wt.% Am-MWCNT/SPES (d), and 0.5 wt.% az-MWCNT/SPES (e).

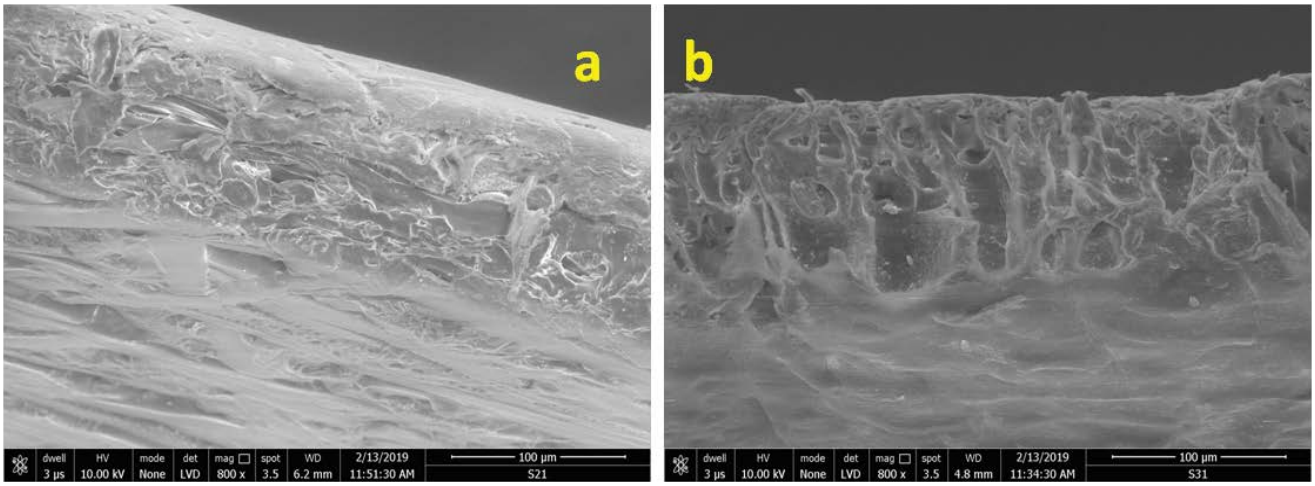

Fig. S5. FE-SEM image of cross-section of pristine SPES (a) and 1 wt.% Am-MWCNT/SPES membranes (b).

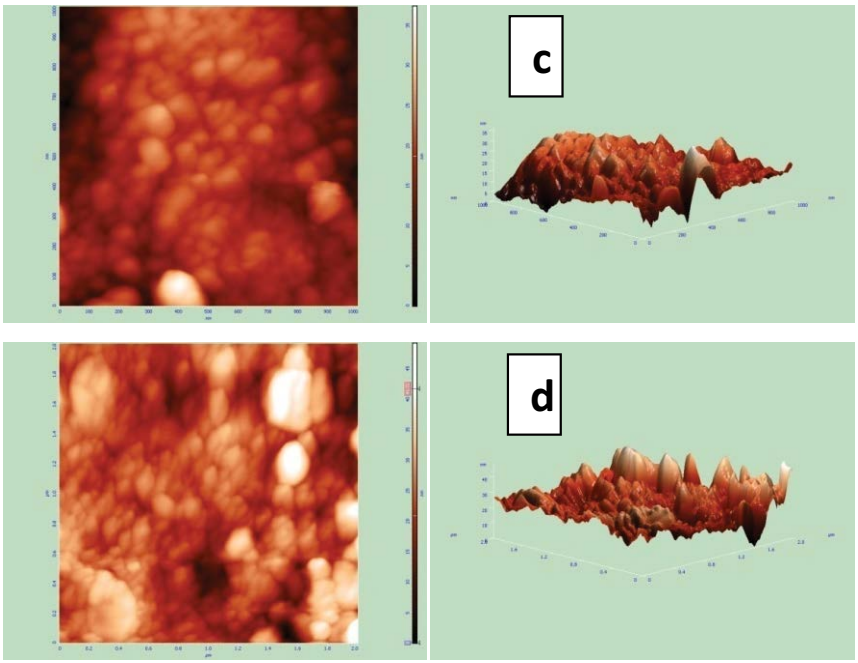

Fig. S6. AFM images of 0.1 wt.% Az-MWCNT/SPES (c) and 0.5 wt.% Az-MWCNT/SPES (d).

Table S3
Pure water flux values of the membranes at different pressure

Membrane	Pure water flux (L/m²h)	
	71 psi	98 psi
S201	171.31	190.11
S205	222.1	252.59
S301	269.30	293.12
S305	304.52	334.59
S401	301.23	320.21
S405	330.71	371.15

Table S4
BSA rejection and fouling ratio of the SPES/f-MWCNT mixed matrix membranes

Membrane	Bovine serum albumin		
	Rejection (%)	Flux recovery ratio (%)	Irreversible fouling ratio (%)
S205	83.1 ± 2.7	69.1 ± 1.3	30.9 ± 1.6
S305	90.4 ± 2.6	75.6 ± 1.6	24.4 ± 2.5
S405	90.9 ± 1.5	78.4 ± 2.5	21.6 ± 4.1

Reference

[S1] D. Lu, H. Zou, R. Guan, H. Dai, L. Li, Sulfonation of polyethersulfone by chlorosulfonic acid, Polym. Bull., 54 (2005) 21–28.